Supporting Information

Bacteria make a living breathing the nitro-heterocyclic insensitive munitions compound 3-nitro-1,2,4-triazol-5-one (NTO)

Camila L. Madeira [1, ⊥], Osmar Menezes [1, 2, ⊥], Doyoung Park [3, ⊥], Kalyani V. Jog [1], Janet K. Hatt [3], Savia Gavazza [2], Mark J. Krzmarzick [4], Reyes Sierra-Alvarez [1], Jim C. Spain [3, 5], Konstantinos T. Konstantinidis [3], Jim A. Field [1*]

[1] Department of Chemical and Environmental Engineering, University of Arizona, Tucson, AZ 85721-0011, USA

[2] Laboratório de Saneamento Ambiental, Departamento de Engenharia Civil e Ambiental, Universidade Federal de Pernambuco, Recife, PE, 50740-530, Brazil

[3] School of Civil and Environmental Engineering, Georgia Institute of Technology, Atlanta, GA 30332-0355, USA

[4] School of Civil and Environmental Engineering, Oklahoma State University, Stillwater, OK 74078, USA

[5] Center for Environmental Diagnostics & Bioremediation, University of West Florida, Pensacola, FL 32514, USA

[⊥] These authors contributed equally to this work.

* Author to whom correspondence should be addressed (jimfield@email.arizona.edu).

Analytical methods

A) HPLC: The concentrations of NTO and ATO were measured using high performance liquid chromatography (HPLC). An Agilent 1290 Infinity HPLC (Santa Clara, CA, USA) coupled with a diode array detector (DAD) was equipped with a Hypercarb column (Thermo Scientific, Waltham, MA, USA), and the mobile phase consisted of a gradient of water with 0.1% trifluoroacetic acid and acetonitrile, as previously described (Madeira et al, 2017).

B) GC-TCD and GC-FID: For CO_2 and acetate analyses, we used a gas chromatograph GC 7890A (Agilent Technologies, Santa Clara, CA, USA) equipped with two detectors and two columns. For CO_2, we used a Carboxen 1010 Plot column (30 m × 0.32 mm, Sigma-Aldrich, St. Louis, MO, USA) and a thermal conductivity detector (TCD) at 230^{o}C. The inlet was operated in splitless mode at 100^{o}C, and the oven temperature was also 100^{o}C. Helium was used as carrier gas at a flow rate of 7 mL/min, and the gas injections of 100 µL were performed with a gastight syringe. For acetate, we used a fused silica Stabilwax®-DA column (30 m × 0.53 mm, Restek, State College, PA, USA) and a flame ionization detector (FID) at 280^{o}C, with air and hydrogen as the flame source. The inlet temperature was 280^{o}C, and the oven temperature started at 100^{o}C, increased to 150^{o}C at a rate of 8^{o}C/min. Helium was used as the carrier gas at a flow rate of 5.2 mL/min, and the injection volume was 1 µL.

C) OD600: The optical density at 600 nm (OD600) was measured at the wavelength of 600 nm using a UV-1800 UV-VIS spectrophotometer (Shimadzu, Kyoto, Japan).

D) ATP: We measured the bioluminescence produced in the ATP assay using a FlexStation 3

multi-mode microplate reader (Molecular Devices, San Jose, CA, USA). The data was analyzed with the ready-to-glow protocol from the software SoftMax Pro 5.2 (also from Molecular Devices) with an integration time of 1500 ms.

Additional experiments

A) Biomass x OD600: Bottles containing different concentrations of substrates and the enrichment culture were incubated, and after the complete reduction of NTO was observed, samples of the suspension were taken for OD600 analysis. The remaining suspension of each bottle was filtered using a 0.22 µm membrane. The filters were dried at 105ºC for 3 hours, and the weight of the dry mass was recorded. The same procedure was performed for abiotic controls. The dry mass obtained for the abiotic controls was subtracted from the dry mass of the biotic treatment to account for inorganic solids. A correlation was established for the OD600 and biomass ($R^2 = 0.9639$), as shown in Figure S1.

B) Use of alternative electron acceptors and electron donors: We assessed the ability of our enrichment culture to use different combinations of electron acceptors and electron donors in closed-bottle experiments. For the experiments using alternative electron acceptors, the enrichment culture (4% v/v) was incubated in mineral medium containing 2000 µM acetate, except for the experiment with ferric citrate, in which case we used 1000 µM acetate. All the bottles were flushed with 80% N_2 / 20% CO_2. The electron acceptors were added to the bottles through concentrated stock solutions to final concentrations oSf 1000 µM for 4-nitroimidazole, 2-methyl-4(5)-nitroimidazole, 4-nitroanisole, 4-nitrophenol, 2,4-dinitrotoluene, nitroguanidine, 3-nitrotriazole, 3-nitripyrazole, and 3000 µM for NO_3^-. In the treatment containing O_2, the bottles

were not flushed, so the partial pressure of O_2 was the same as in the atmosphere. For the experiments using alternative electron donors, the enrichment culture (4% v/v) was incubated in mineral medium containing 1000 µM NTO. Glucose and ethanol were added through stock solutions to final concentrations of 500 and 1000 µM, respectively. In the treatment containing hydrogen, 10 mL of pure H_2 were added to the sealed bottles using a syringe. The total suspension volume was 50 mL, and the bottles were kept in the dark in an orbital shaker at 130 rpm and 30°C. In the experiments using alternative electron acceptors, we assessed the disappearance of the nitro-containing compounds via HPLC measurements or the disappearance of acetate via GC measurements. In the experiments testing the use of alternative electron donors, we assessed the disappearance of NTO over time. All the samples were clarified by centrifugation prior to analysis.

We tested the ability of our culture to reduce NTO in the presence of O_2 and NO_3^-. The experiments were performed as previously described, with an NTO concentration of 1000 µM, and an acetate concentration of 2000 µM for the experiment with O_2 and 4000 µM for the experiment with NO_3^-. For the treatment with O_2, pure O_2 was added to the sealed bottles with a syringe to a final concentration of 2 mg L^{-1} dissolved oxygen, and in the treatment with NO_3^-, the final NO_3^- concentration was 5000 µM.

We also tested the ability of our enrichment culture to reduce Fe(III) in the form of soluble ferric citrate. The enrichment culture (2% v/v) was incubated in mineral medium containing 500 µM ferric citrate and 1000 µM acetate. The total volume of the suspension was 50 mL, and the headspace was flushed with 80% N_2 / 20% CO_2 to create anaerobic conditions. Additionally, we had a control without acetate (Fe(III) + EC) and an abiotic control (Fe(III) + Ac). The bottles were kept in the dark in a shaker at 130 rpm and 30°C. Samples taken over time were acidified to prevent Fe(II) oxidation and then clarified by centrifugation. The increase in Fe(II) concentration over time

was assessed using the Ferrozine method (Stookey, 1970).

C) Effect of iron concentration on NTO reduction rate: To investigate the use of Fe by the enrichment culture (2% v/v) as a redox mediator for NTO reduction, we conducted an experiment with different added Fe(II) concentrations in the medium (0.0, 0.6, and 1.8 mg L^{-1}) as ferrous chloride. The NTO and acetate concentrations were both 1000 µM. The experiment was conducted in closed bottles as previously described, and the NTO concentration was measured over time. Liquid samples were taken after the complete removal of NTO for soluble Fe analysis by ICP-OES. These samples were clarified and acidified to a final concentration of 2% (v/v) nitric acid prior to the analysis.

Metagenomic analysis

A) DNA extraction: DNA was extracted by using a phenol-chloroform extraction as previously described [1] with minor modifications. One-fourth of the filter was placed in a microcentrifuge tube with lysis buffer (50 mM Tris−HCl pH 8.3, 40 mM EDTA, and 0.75 M sucrose), and the cells were disrupted with a mini bead beater 24 (BioSpec Products, Bartlesville, OK) at maximum speed twice for one minute each time, with icing in between. DNA samples from technical replicates were pooled for sequencing.

B) DNA sequencing: DNA sequencing libraries were prepared using Illumina's Nextera XT DNA library prep kit according to the manufacturer's protocol, except that the protocol was terminated after isolation of cleaned double-stranded libraries. Library concentrations were measured using a Qubit HS DNA assay and Qubit 2.0 fluorometer (Thermo Fisher Scientific). To determine library

insert sizes, library samples were run on a 2100 Bioanalyzer instrument (Agilent) using the High Sensitivity DNA chip. The NTO metagenomic library was sequenced on an Illumina MiSEQ for 500 cycles (2 x 250-bp paired-end) in the Georgia Institute of Technology Molecular Evolution Core facility. Adapter trimming and de-multiplexing were carried out on each instrument.

C) Quality control and assembly: Illumina sequence reads of the enrichment culture metagenome was trimmed and read quality was assessed by using FaQCs with a minimum cut-off of Q=30 (99.9% accuracy per base-position) with length of 50 bp[2]. The trimmed reads passing these cut-offs were assembled using IDBA-UD v 1.1.1[3] with default options for each metagenome; scripts of the enveomics collection[4] were used to prepare the data and process the resulting assembly files.

D) Sequence coverage: To assess the sequencing coverage of the sampled enrichment culture by metagenome sequencing, i.e., what percent of the total community was sequenced, Nonpareil version 3.303 with default settings and the alignment algorithm[5] was used. The underlying statistics are summarized in Table S2 and the results of Nonpareil in Figure S5.

E) 16S rRNA gene fragment analysis: Extraction of the V4 region of the 16S rRNA (16S) genes from metagenomic reads followed the procedure described in Johnston *et al.*[6] with minor modifications. Specifically, to obtain a reference V4 region database for searching against the metagenomic reads, 16S V4 region primers[7] were aligned *in silico* against the GreenGenes 16S full-length database (May 2013 version) by running blastn[8]. Then, the sequences which matched both the forward and reverse primers with over 90% nucleotide identity were selected. The selected sequences were trimmed to include only the V4 region (not upstream or downstream sequences),

and the curated V4 region sequences were used as the reference database. Subsequently, metagenome reads were searched against the curated V4 region database by using blastn with -task megablast, -word_size 19 options[8, 9]. The best database match for each read was identified when the read had better than 70% nucleotide sequence identity and the read was trimmed as described above to include only the V4 region. The trimmed reads were used as input for QIIME2 and analyzed using the *de novo* clustering method[10]. The reads were dereplicated using the vsearch dereplicate-sequences command and clustered in Operational Taxonomic Units (OTUs) based on the 97% of sequence identity with the cluster-features-de-novo --p-perc-identity 0.97[11] command. Taxonomic annotation of 97% nucleotide identity-based OTUs was performed with the feature-classifier plugin by using SILVA database[12] as implemented in QIIME 2 (Silva_132_97_16S.qza file).

F) Finding rRNA genes of MAGs: rRNA genes in the MAGs were identified with blast searches against the RDP database release 11.5[13]. The sequences of the MAGs were aligned against the RDP database by using blastn with -max_target_seqs 4 option[8]. The blast results were filtered by 97% nucleotide identity and the best matches were selected

Consortium composition based on 16S rRNA gene sequence fragments

Coverage of all sampled consortia by metagenomic sequencing assessed by Nonpareil was in the range of 95.54% to 98.29%, indicating that nearly the whole consortium was covered by sequencing, and only a few, rare members were not well represented in our sequencing results (Figure S6). 93 OTUs were found in the NTO metagenome by analyzing the 16S rRNA gene V4 region, but only six of them showed total relative abundance higher than 1% (Figure S7). At the genus level, four OTUs assigned to the *Geobacter* genus were predominant, showing a cumulative

71.4% of relative abundance. The second most dominant taxon was assignable to the *Betaproteobacteriales* order consisting of two OTUs and 10.5% of the sample's relative abundance.

Population genome binning was performed with MaxBin 2.0 on the metagenome of the enrichment culture to assess the community composition at the genome level and elucidate the total genetic potential of the consortia. Two MAGs were recovered in the NTO metagenome. The quality of the MAGs was assessed based on the quality score from MiGA calculated as "completeness – 5 × contamination" estimated based on essential genes[14]. The quality of all the MAGs was high, showing scores of 90.5 for MAG1 and 84.2 for MAG2 (Table 1).

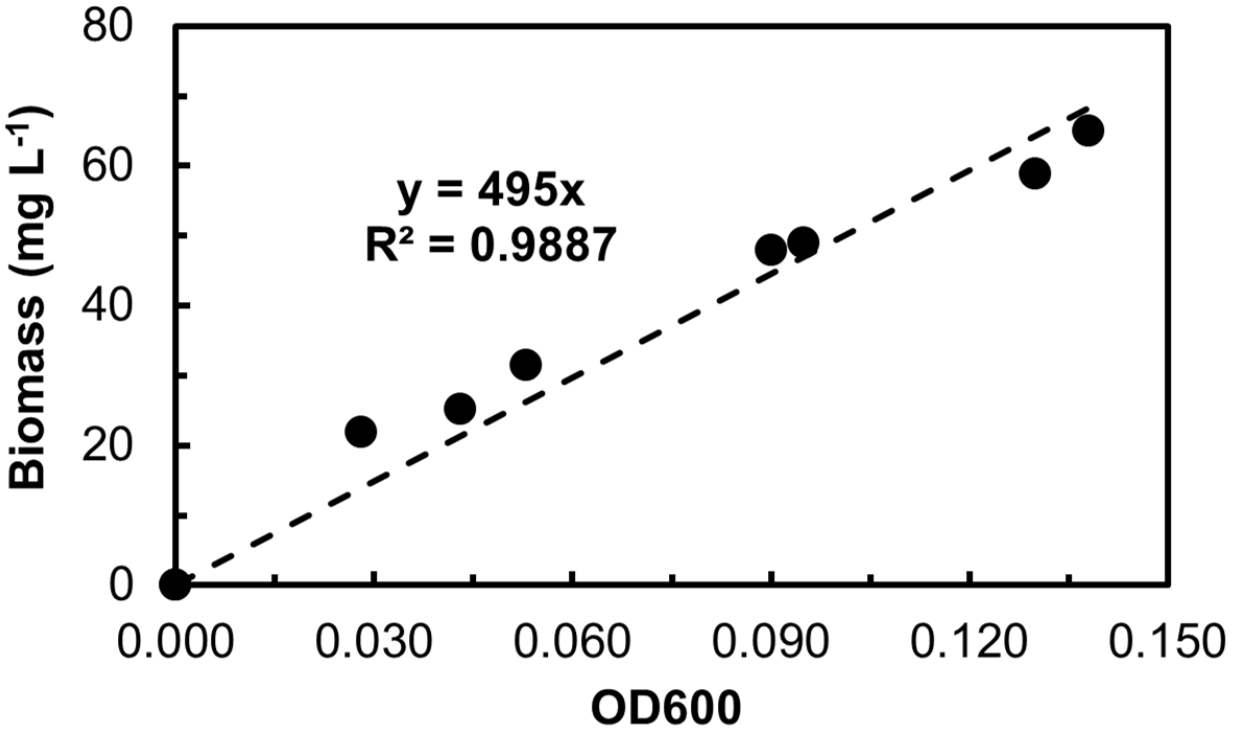

Figure S1. Correlation between optical density at 600 nm (OD600) and biomass production by the NTO-acetate enrichment culture (mg VSS L^{-1}) after complete reduction of different concentrations of NTO.

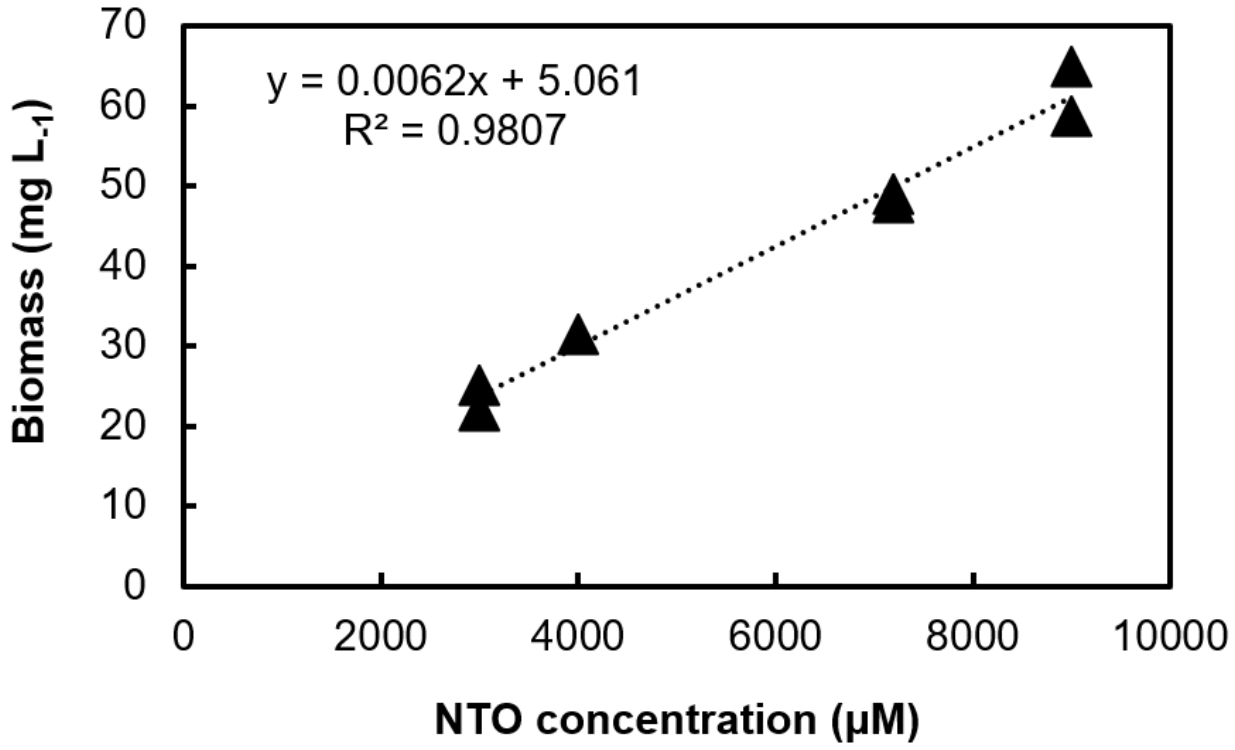

Figure S2. Correlation between NTO concentration and biomass production by the NTO-acetate enrichment culture (mg VSS L^{-1}) after complete NTO reduction in mineral medium containing a 2-fold excess of acetate for each NTO concentration.

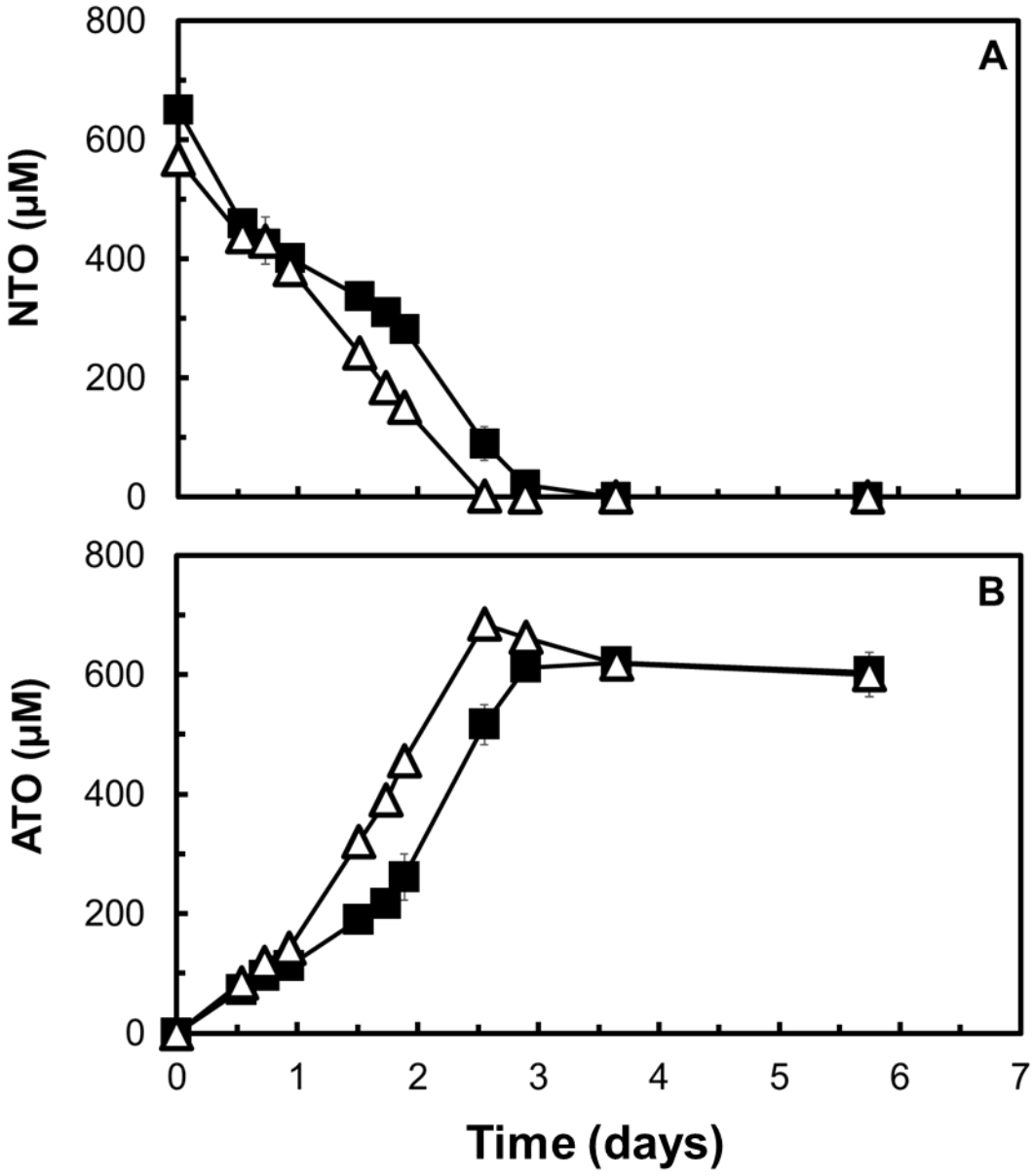

Figure S3. NTO reduction to ATO by municipal anaerobic digester sludge was not significantly affected by CCCP addition at a concentration of 0.6 mg L^{-1}. Legend: Sludge + NTO + acetate (△), sludge + NTO + acetate + CCCP (■). Symbols represent the average of three replicates, and error bars represent the standard deviation.

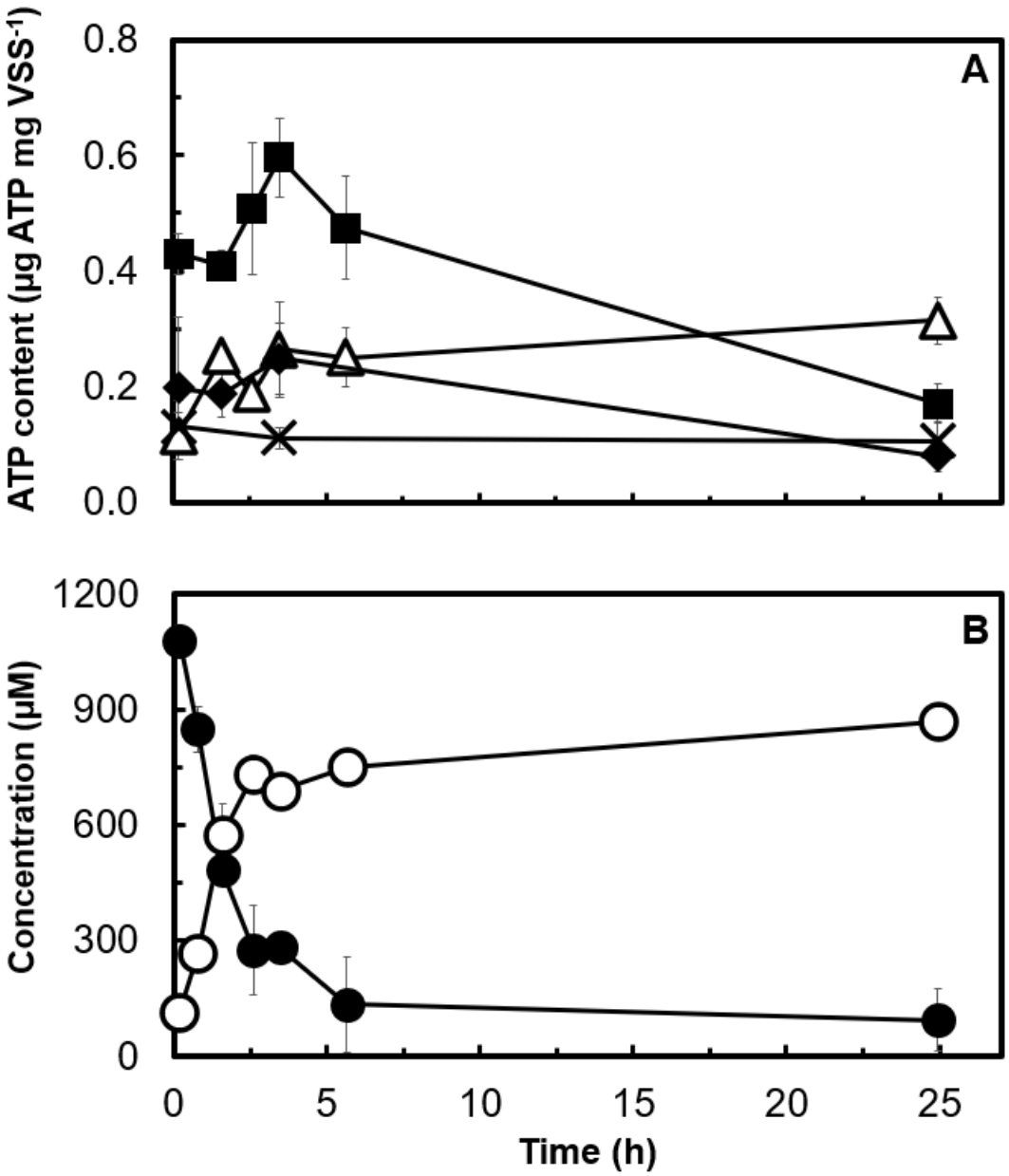

Figure S4. ATP production of the enrichment culture incubated with NTO and acetate. Panel A: ATP production in different incubation conditions. Panel B: NTO consumption and ATO formation by the enrichment culture incubated with both NTO and acetate. Legend: EC + NTO + acetate (■), EC + acetate (△), EC + NTO (⧫), EC (✕), NTO concentration (●), and ATO concentration (○). Symbols represent the average of three replicates, and error bars represent the standard deviation.

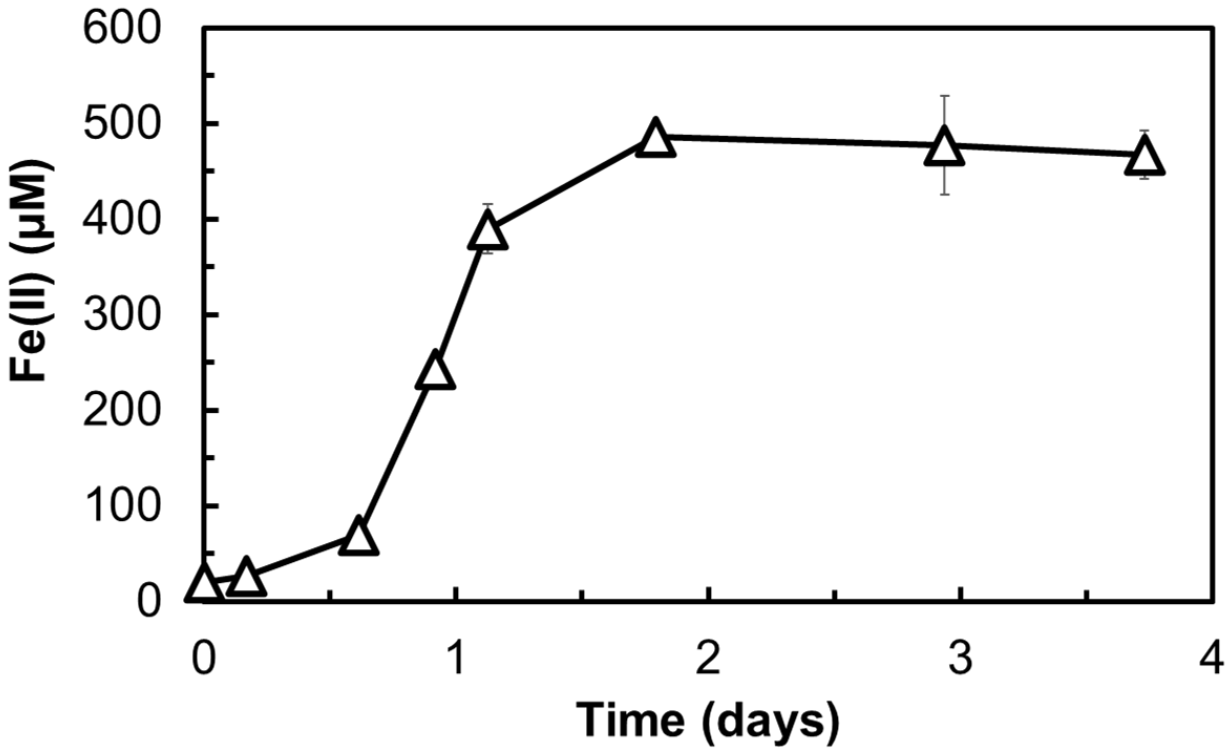

Figure S5. Production of Fe (II) (△) by the enrichment culture incubated with ferric citrate (500 µM) and acetate (1000 µM). Symbols represent the average of three replicates, and error bars represent the standard deviation.

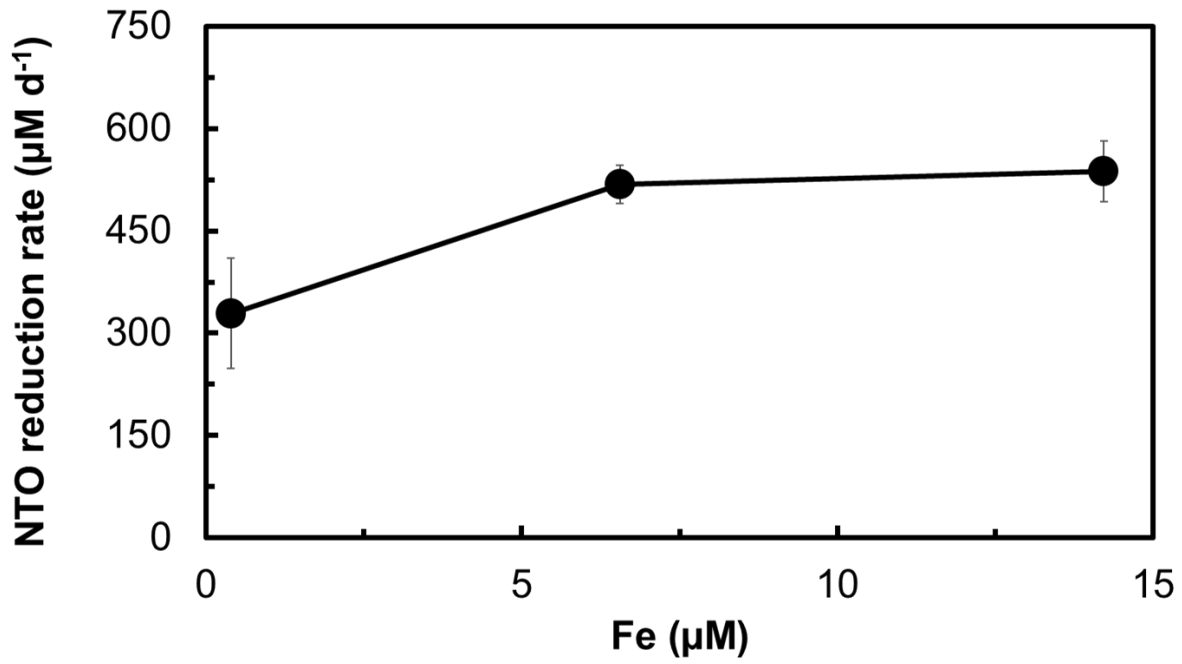

Figure S6. Rate of NTO reduction by the enrichment culture versus total Fe concentration measured in the medium. The added Fe concentrations were 0.0, 0.6, and 1.8 mg L^{-1}. Symbols represent the average of three replicates, and error bars represent the standard deviation.

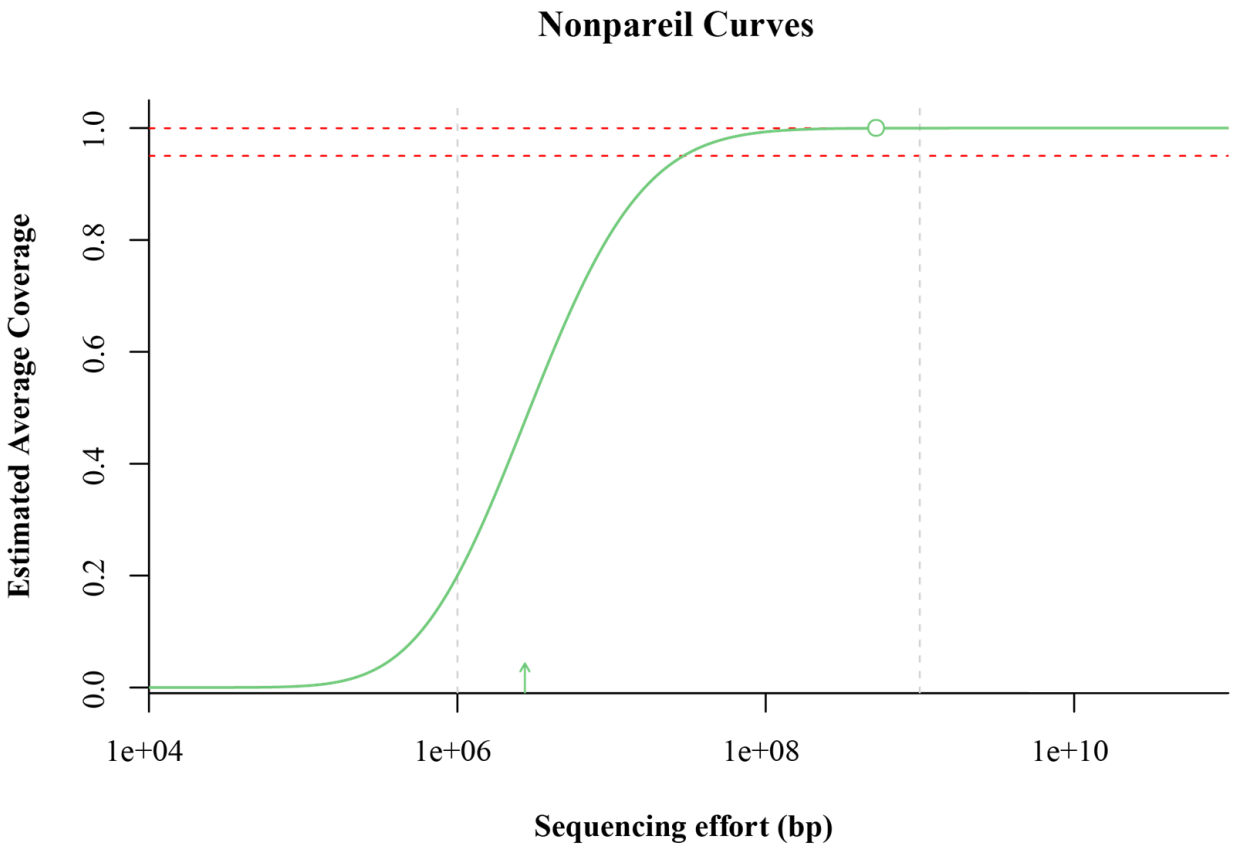

Figure S7. Coverage of the metagenome and microbial community complexity as assessed by Nonpareil. Nonpareil is a tool that estimates datasets complexity and sequencing effort needed to achieve to desired level by using read redundancy. Circle represents estimated coverage obtained; the line to the right of the circle represent projection to complete (100%) coverage. The dashed lines represent 95% and 99% of coverage respectively. The arrows represent the sequencing effort required for achieving 50% of coverage.

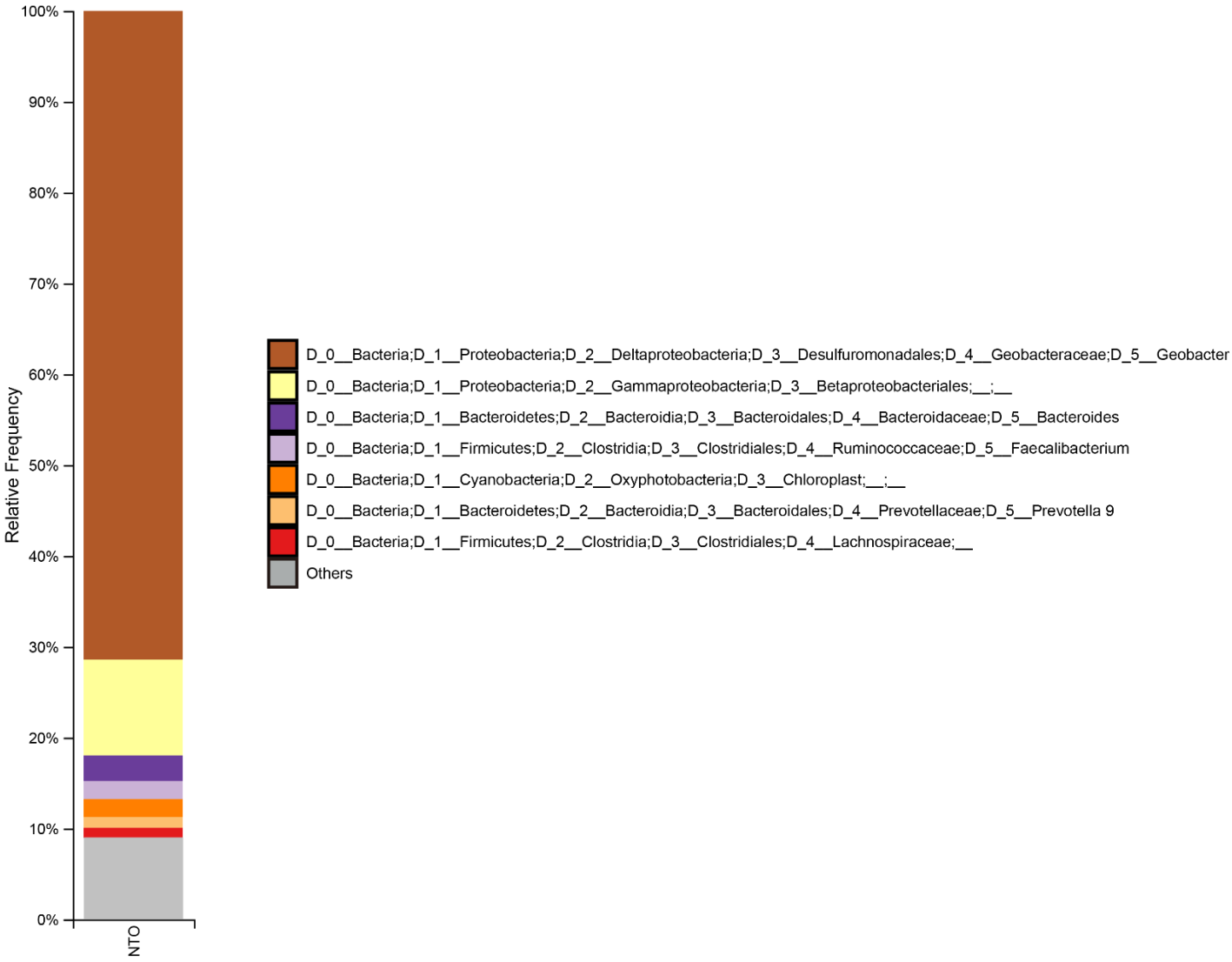

Figure S8. Relative abundance of 16S rRNA V4 region gene-based OTUs at the genus level. OTUs recovered from the NTO metagenome were analyzed using the Qiime2 pipeline as described in the Materials and Methods section.

Table S1. Cell growth of the NTO-acetate enrichment culture incubated with different combinations of electron donors and electron acceptors.

e^- Acceptor	e^- Donor	e^- Acceptor reduction observed
NTO	Acetate	Yes
4-Nitroimidazole	Acetate	No
2-Methyl-4(5)-nitroimidazole	Acetate	No
4-Nitroanisole	Acetate	No
4-Nitrophenol	Acetate	No
2,4-Dinitrotoluene	Acetate	No
2,4-Dinitroanisole	Acetate	No
Nitroguanidine	Acetate	No
3-Nitrotriazole	Acetate	No
3-Nitropyrazole	Acetate	No
Ferric citrate	Acetate	Yes
O_2	Acetate	Yes
NO_3^-	Acetate	Yes
NTO	Glucose	Yes
NTO	H_2	No
NTO	Ethanol	No

Table S2. Statistics of the metagenome used in this study.

Trimming results	
Average raw length (bp)	204.3
Raw reads (million reads)	6.5
Average trimmed length (bp)	177.6
Trimmed reads (million reads)	5.7
Assembly results	
N50 (bp)	27244
Sequences	652
Total length (Mb)	7.6
V4 region fragments	963

Table S3. Geobacter MAG1 cytochrome content based on bioinformatics gene functional prediction.

	No. in MAG1
ORFs in genome	3429
Cytochromes total	115
Cytochromes (% genome)	3.4
multi heme cytochromes	63
Cytochromes (% multiheme)	54.8
Avg. hemes per cytochrome	4.92

Table S4. Candidate nitroreductases for NTO reduction to ATO and their best match homolog.

MAG	AA length (Alignment)	Identity	Closest hit	Accession	DB
MAG1_45_15	149	35.6	*Archaeoglobus fulgidus*	O28017	SwissProt
MAG1_11_118	176	35.2	*Archaeoglobus fulgidus*	O30013	SwissProt
MAG1_2_47	193	34.2	*Archaeoglobus fulgidus*	O30013	SwissProt
MAG2_73_5	466	53.4	*Pseudomonas putida*	Q88K03	SwissProt
MAG2_139_5	220	39.5	*Pseudomonas oleovorans*	Q6DLR9	SwissProt

Table S5. Proposed *Geobacter* MAG1 EET (extracellular electron transfer system) content based on bioinformatics gene functional prediction.

CytC Family ID[30]	Genetic code	Best hit gene description in NCBI	No of ORFs in family	No of CXXCH	Estimated location
2568	macA family	cytochrome C peroxidase	1	2	Inner Membrane
1467	cbcL family	cytochrome C	1	9	Inner Membrane
49	ppcA family	cytochrome C3 family protein	1	3	Periplasm
3948	ppcD family	cytochrome C3 family protein	1	3	Periplasm
3353	ppcE family	cytochrome C3 family protein	1	3	Periplasm
1653	omcB family	C-type polyhemecytochrome OmcB	1	4	Outer Membrane
51	omaB family	cytochrome C	1	8	Periplasm/Outer Membrane
2177	omcE family	cytochrome C3 family protein	1	4	Outer Membrane
1292	omcQ family	cytochrome C3 family protein	1	12	Outer Membrane
64	omcS family	C-type cytochrome OmcS, hypothetical protein	3	6	Outer Membrane
2504	omcX family	cytochrome C	1	12	Outer Membrane
1253	omcY family	cytochrome C	1	8	Outer Membrane
2307	omcZ family	cytochrome C	2	7	Outer Membrane
1964	cbcA family	cytochrome C	1	7	Periplasm/Outer Membrane

References

1. Tsementzi, D.; Rodriguez-R, L. M.; Ruiz-Perez, C. A.; Meziti, A.; Hatt, J. K.; Konstantinidis, K. T., Ecogenomic characterization of widespread, closely-related SAR11 clades of the freshwater genus "Candidatus Fonsibacter" and proposal of Ca. Fonsibacter lacus sp. nov. *Systematic and Applied Microbiology* **2019,** *42*, (4), 495-505.
2. Lo, C.-C.; Chain, P. S. G., Rapid evaluation and quality control of next generation sequencing data with FaQCs. *BMC Bioinformatics* **2014,** *15*, (1), 366.
3. Peng, Y.; Leung, H. C.; Yiu, S.-M.; Chin, F. Y., IDBA-UD: a de novo assembler for single-cell and metagenomic sequencing data with highly uneven depth. *Bioinformatics* **2012,** *28*, (11), 1420-1428.
4. Rodriguez-R, L. M.; Konstantinidis, K. T. *The enveomics collection: a toolbox for specialized analyses of microbial genomes and metagenomes*; 2167-9843; PeerJ Preprints: 2016.
5. Rodriguez-R, L. M.; Gunturu, S.; Tiedje, J. M.; Cole, J. R.; Konstantinidis, K. T., Nonpareil 3: Fast Estimation of Metagenomic Coverage and Sequence Diversity. *mSystems* **2018,** *3*, (3), e00039-18.
6. Johnston, E. R.; Rodriguez-R, L. M.; Luo, C.; Yuan, M. M.; Wu, L.; He, Z.; Schuur, E. A.; Luo, Y.; Tiedje, J. M.; Zhou, J., Metagenomics reveals pervasive bacterial populations and reduced community diversity across the Alaska tundra ecosystem. *Frontiers in microbiology* **2016,** *7*, 579.
7. McDonald, D.; Price, M. N.; Goodrich, J.; Nawrocki, E. P.; DeSantis, T. Z.; Probst, A.; Andersen, G. L.; Knight, R.; Hugenholtz, P., An improved Greengenes taxonomy with explicit ranks for ecological and evolutionary analyses of bacteria and archaea. *The ISME journal* **2012,** *6*, (3), 610.
8. Camacho, C.; Coulouris, G.; Avagyan, V.; Ma, N.; Papadopoulos, J.; Bealer, K.; Madden, T. L., BLAST+: architecture and applications. *BMC bioinformatics* **2009,** *10*, (1), 421.
9. Altschul, S. F.; Gish, W.; Miller, W.; Myers, E. W.; Lipman, D. J., Basic local alignment search tool. *Journal of Molecular Biology* **1990,** *215*, (3), 403-410.
10. Bolyen, E.; Rideout, J. R.; Dillon, M. R.; Bokulich, N. A.; Abnet, C. C.; Al-Ghalith, G. A.; Alexander, H.; Alm, E. J.; Arumugam, M.; Asnicar, F.; Bai, Y.; Bisanz, J. E.; Bittinger, K.; Brejnrod, A.; Brislawn, C. J.; Brown, C. T.; Callahan, B. J.; Caraballo-Rodríguez, A. M.; Chase, J.; Cope, E. K.; Da Silva, R.; Diener, C.; Dorrestein, P. C.; Douglas, G. M.; Durall, D. M.; Duvallet, C.; Edwardson, C. F.; Ernst, M.; Estaki, M.; Fouquier, J.; Gauglitz, J. M.; Gibbons, S. M.; Gibson, D. L.; Gonzalez, A.; Gorlick, K.; Guo, J.; Hillmann, B.; Holmes, S.; Holste, H.; Huttenhower, C.; Huttley, G. A.; Janssen, S.; Jarmusch, A. K.; Jiang, L.; Kaehler, B. D.; Kang, K. B.; Keefe, C. R.; Keim, P.; Kelley, S. T.; Knights, D.; Koester, I.; Kosciolek, T.; Kreps, J.; Langille, M. G. I.; Lee, J.; Ley, R.; Liu, Y.-X.; Loftfield, E.; Lozupone, C.; Maher, M.; Marotz, C.; Martin, B. D.; McDonald, D.; McIver, L. J.; Melnik, A. V.; Metcalf, J. L.; Morgan, S. C.; Morton, J. T.; Naimey, A. T.; Navas-Molina, J. A.; Nothias, L. F.; Orchanian, S. B.; Pearson, T.; Peoples, S. L.; Petras, D.; Preuss, M. L.; Pruesse, E.; Rasmussen, L. B.; Rivers, A.; Robeson, M. S.; Rosenthal, P.; Segata, N.; Shaffer, M.; Shiffer, A.; Sinha, R.; Song, S. J.; Spear, J. R.; Swafford, A. D.; Thompson, L. R.; Torres, P. J.; Trinh, P.; Tripathi, A.; Turnbaugh, P. J.; Ul-Hasan, S.; van der Hooft, J. J. J.; Vargas, F.; Vázquez-Baeza, Y.; Vogtmann, E.; von Hippel, M.; Walters, W.; Wan, Y.; Wang, M.; Warren, J.; Weber, K. C.; Williamson, C. H. D.; Willis, A. D.; Xu, Z. Z.; Zaneveld, J. R.; Zhang, Y.; Zhu, Q.; Knight, R.; Caporaso, J. G., Reproducible, interactive, scalable and extensible microbiome data science using QIIME 2. *Nature Biotechnology* **2019,** *37*, (8), 852-857.

11. Rognes, T.; Flouri, T.; Nichols, B.; Quince, C.; Mahé, F., VSEARCH: a versatile open source tool for metagenomics. *PeerJ* **2016,** *4*, e2584.
12. Quast, C.; Pruesse, E.; Yilmaz, P.; Gerken, J.; Schweer, T.; Yarza, P.; Peplies, J.; Glöckner, F. O., The SILVA ribosomal RNA gene database project: improved data processing and web-based tools. *Nucleic acids research* **2012,** *41*, (D1), D590-D596.
13. Cole, J. R.; Wang, Q.; Fish, J. A.; Chai, B.; McGarrell, D. M.; Sun, Y.; Brown, C. T.; Porras-Alfaro, A.; Kuske, C. R.; Tiedje, J. M., Ribosomal Database Project: data and tools for high throughput rRNA analysis. *Nucleic acids research* **2014,** *42*, (Database issue), D633-D642.
14. Rodriguez-R, L. M.; Gunturu, S.; Harvey, W. T.; Rosselló-Mora, R.; Tiedje, J. M.; Cole, J. R.; Konstantinidis, K. T., The Microbial Genomes Atlas (MiGA) webserver: taxonomic and gene diversity analysis of Archaea and Bacteria at the whole genome level. *Nucleic acids research* **2018,** *46*, (W1), W282-W288.